J Mater Sci: Mater Electron (2017) 28:2200–2205
DOI 10.1007/s10854-016-5786-5

Strontium molybdate nanostructures: synthesis of different shapes through a new approach and its photocatalyst application

Mehdi Rahimi-Nasrabadi[1,2]

Received: 21 July 2016 / Accepted: 3 October 2016 / Published online: 8 October 2016

Abstract A new method is described for synthesizing flower-like strontium molybdate nanostructures by strontium nitrate hexahydrate and ammonium heptamolybdate tetrahydrate as starting materials and in the presence of amino acids as of capping agents. The effect of different amino acids such as phenylalanine, glycine, and cysteine on the size and morphology of Strontium molybdate ($SrMoO_4$) nanostructures were investigated. According to the vibrating sample magnetometer, $SrMoO_4$ nanostructures indicated a ferromagnetic behavior at room temperature. The stages of the formation of $SrMoO_4$, as well as the characterization of the resulting compounds were done using X-ray diffraction, scanning electron microscopy, diffuse reflectance spectroscopy (UV–Vis), and energy dispersive X-ray microanalysis. The products were analyzed by transmission electron microscopy and ultraviolet–visible (UV–Vis) spectroscopy to be, about 30–50 nm in size and $E_g = 2.10$ eV.

1 Introduction

Materials at the nanometer scale have been studied for decades because of their unique properties arising from the large fraction of atoms residing on the surface, and also from the finite number of atoms in each crystalline core. Especially, because of the increasing need for high area density storage, the synthesis and characterization of semiconductor nanocrystals have been extensively investigated [1–10]. Scheelite-structured compounds belonging to the molybdate and tungstate families possess attractive luminescence and interesting structural properties. Because of their physical and chemical properties they are used in several technological applications. In particular, laser-host materials [11], scheelite-type crystals are used as scintillators [12], cryogenic detectors for dark matter [13], or heterogeneous catalysts [14]. Alkaline-earth molybdates form part of these compounds. They produce green luminescence required for the uses of electro-optical devices [15] and recent studies have shown that these molybdate crystals have good prospects as possible negative electrode materials to replace the graphite presently being used in the Li-ion batteries [16]. On top of that, scheelite molybdates and tungstates are also being considered for the development of eye-safe Raman lasers [17]. Understanding the electro-optical and structural properties of these compounds is very important for the above mentioned applications. Various approaches have been used to prepare these materials, involving solid-state reaction [18], molten salt route [19], microwave-assisted citrate complex method [20], solvothermal synthesis [21], complex polymerization [22], reverse microemulsion process [23], electrochemical method [24], and combustion synthesis [25]. Among all these approaches, co-precipitation process has confirmed a successful approach to prepare inorganic nanomaterials with interesting morphologies and regular particle sizes. In this work, we report the synthesis and characterization of $SrMoO_4$ nanostructures through the precipitation method. Besides, several experiments were performed in order to investigate the effect of different amino acids such as phenylalanine, glycine, and cysteine on the morphology and particle size of final products. By selecting the

✉ Mehdi Rahimi-Nasrabadi
Rahiminasrabadi@gmail.com

[1] Faculty of Pharmacy, Baqiyatallah University of Medical Sciences, Tehran, Iran

[2] Department of Chemistry, Imam Hossein University, Tehran, Iran

suitable capping agent and starting materials the well-known precipitation method can be an excellent procedure to produce the nanocrystalline $SrMoO_4$ powders [26–30].

2 Experimental

2.1 Materials

Methylene orange was of analytical reagent grade quality used without further purification. Other chemicals were commercial products of analytical grade or reagent-grade. All the solutions were prepared with distilled water.

2.2 Characterization

All the chemicals used in this method were of analytical grade and used as-received without any further purification. X-ray diffraction (XRD) patterns were recorded by a Philips-X'PertPro, X-ray diffractometer using Ni-filtered Cu Kα radiation at scan range of $10 < 2\theta < 80$. Scanning electron microscopy (SEM) images were obtained on LEO-1455VP equipped with an energy dispersive X-ray spectroscopy. Spectroscopy analysis (UV–Vis) was carried out using shimadzu UV–Vis scanning UV–Vis diffuse reflectance spectrometer. The energy dispersive spectrometry (EDS) analysis was studied by XL30, Philips microscope. The magnetic measurement of samples were carried out in a vibrating sample magnetometer (VSM; Meghnatis Daghigh Kavir Co.; Kashan Kavir; Iran) at room temperature in an applied magnetic field sweeping between $\pm$ 10,000 Oe.

2.3 Synthesis of $SrMoO_4$ nanostructures

In this study, the synthesis of $SrMoO_4$ was performed by a precipitation approach. Ammonium heptamolybdate tetrahydrate (1 mmol) and $Sr(NO_3)_2{\cdot}6H_2O$ (7 mmol) was dissolved in 60 ml of distilled water separately. Then, amino acids as of capping agents was added to the ammonium heptamolybdate tetrahydrate solution. Subsequently, the solution of $Sr(NO_3)_2{\cdot}6H_2O$ was added into the above solution. Finally, the white precipitate was filtered and washed three times with distilled water. The final product was dried at 90 °C in a conventional furnace in air atmosphere. Reaction conditions are listed in Table 1.

2.4 Photocatalytic experimental

The photocatalytic activities of $SrMoO_4$ nanocrystal were determined by the degradation of aqueous methyl orange (MO) under UV light. About 0.1 g of the sample was first inserted into a reactor that included 50 ppm of aqueous MO. The suspension was transferred into a self-designed glass reactor, and stirred in darkness to attain the adsorption equilibrium. In the research of photo

Table 1 Preparation conditions for the synthesis of $SrMoO_4$ nanostructures

Sample no.	Capping agent	Temperature (°C)	Decolorization (%)
1	Phenylalanine	90	83
2	Glycine	90	–
3	Cysteine	90	–

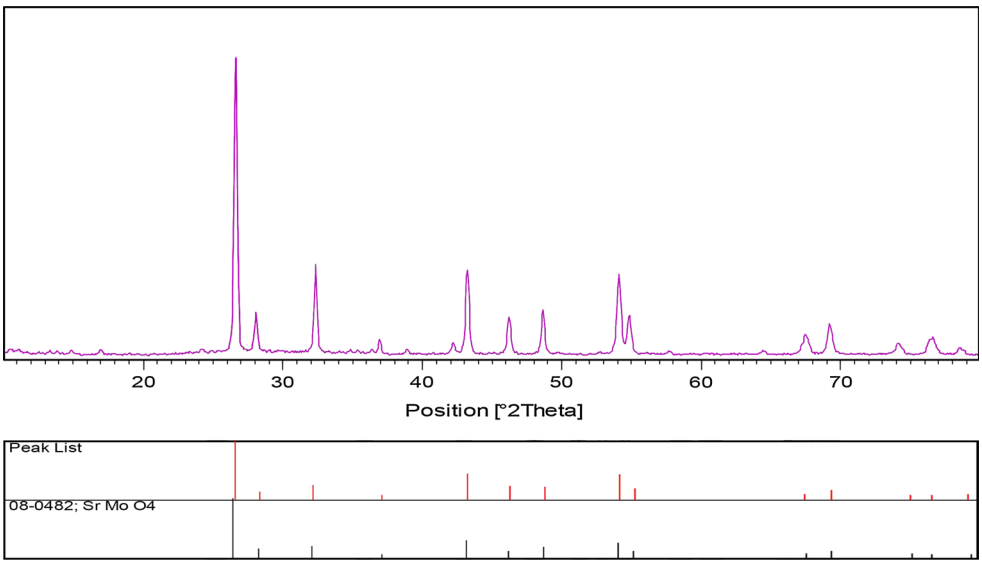

Fig. 1 XRD pattern of $SrMoO_4$ nanostructures (sample 3)

degradation by UV light, a 400 W mercury lamp with a water cooling cylindrical jacket was utilized. The photocatalytic activity of $SrMoO_4$ nanostructure was tested by using methyl orange (MO) solution. The degradation reaction was carried out in a quartz photocatalytic reactor. The photocatalytic degradation was carried out with 50 ppm of MO solution containing 0.1 g of nanostructures. This mixture was aerated for 30 min to reach adsorption equilibrium. Then, the mixture was placed inside the photoreactor in which the vessel was 20 cm away from the UV. The quartz vessel and light sources were placed inside a black box equipped with a fan to prevent UV leakage. Aliquots of the mixture were taken at periodic intervals during the irradiation, and after centrifugation they were analyzed with the UV–Vis spectrometer. The methyl orange (MO) degradation percentage was calculated as:

$$\text{Degradation rate}(\%) = 100\,(C_0 - C_t)/C_0 \quad (1)$$

where A_t and A_0 are the obtained absorbance value of the methyl orange solution at t and 0 min by a UV–vis spectrometer, respectively.

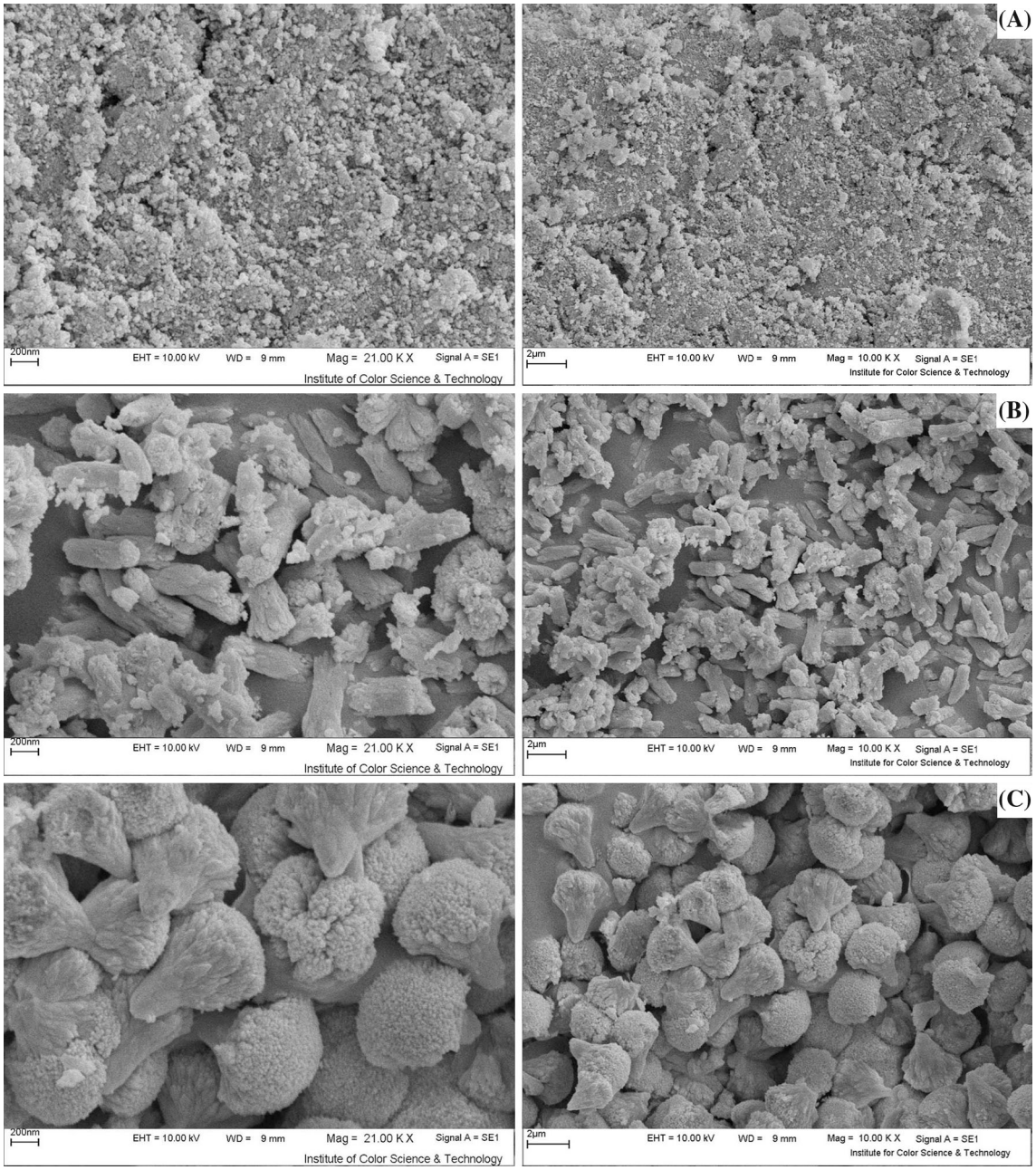

Fig. 2 SEM image of $SrMoO_4$ nanostructures **a** sample 1, **b** sample 2 and **c** sample 3

3 Results and discussion

Crystalline structure and phase purity of as-prepared product has been determined using XRD. The XRD pattern of as-prepared $SrMoO_4$ is shown in Fig. 1. Based on the Fig. 1, the diffraction peaks observed can be indexed to pure tetragonal phase of $SrMoO_4$ with space group of I41/a and JCPDS no. 08-0482. No diffraction peaks from other species could be detected, which indicates the obtained sample is pure. From XRD data, the crystallite diameter (Dc) of $SrMoO_4$ nanostructures was calculated to be 10 nm using the Scherer equation:

$$D_c = K\lambda/\beta\cos\theta \text{ Scherer equation}$$

where β is the breadth of the observed diffraction line at its half intensity maximum (400), K is the so-called shape factor, which usually takes a value of about 0.9, and λ is the wavelength of X-ray source used in XRD. In the third millennium, current studies show that different type of capping agent such as ionic, polymeric; etc. play a fundamental role in synthesis procedures [31–42]. Moreover, capping agents are essential materials for preparation of many disperse systems such as solid/liquid dispersions (usually referred to as suspensions); therefore, in this research we examined the effect of three capping agents such as phenylalanine, glycine, and cysteine on the morphology and particle size of final products. Figure 2a–c shows the SEM images of the sample 1–3, respectively. In the presence of phenylalanine (sample 1, Fig. 2a) the final products mainly consist of nanoparticles with average particle size 30–50 nm. Besides, in the presence of glycine and cysteine as the capping agents the particle size of products were increased and products become In the absence of capping agents (glycine and cysteine), the product mainly consists of flower-like nanostructures which formed by nanostructure, as shown in Fig. 2b, c. The purity of nanocrystalline product was also confirmed by EDS analysis. According to Fig. 3, the sample no. 3 is composed of Sr, Mo and O elements. Furthermore, no impurity peaks are seen, which indicates a high level of purity in the sample. The VSM magnetic measurements for the strontium molybdate oxide (Fig. 4) show the magnetic properties of nanostructures. The $SrMoO_4$ nanostructures exhibit ferromagnetic behaviour at room temperature, with a saturation magnetization of 0.0009 emu/g. Figure 5 shows the $(\alpha h\nu)^2$ versus hy curve of $SrMoO_4$ nanostructures which were calculated from their UV–Vis absorbance using the equation proposed by Wood and Tauc exhibited the equation below.

$$\alpha h\upsilon = (h\nu - Eg)^n \quad (2)$$

where a is the absorbance, h the Planck constant, y the photon frequency, E_g the energy gap, and n the pure

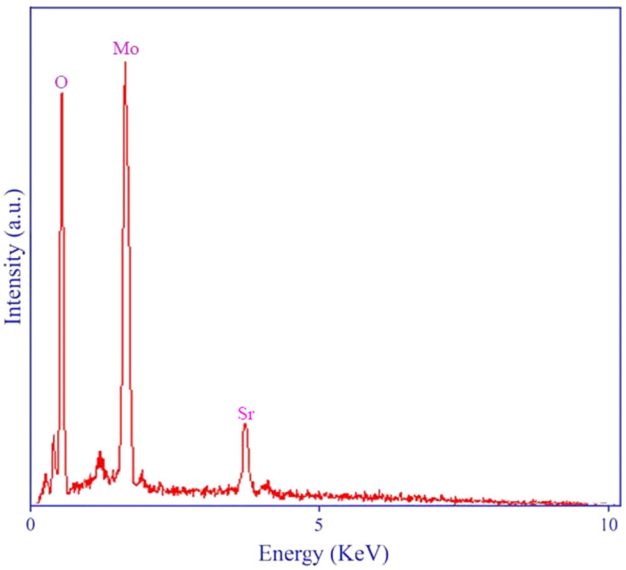

Fig. 3 EDS pattern of $SrMoO_4$ nanostructures (sample 3)

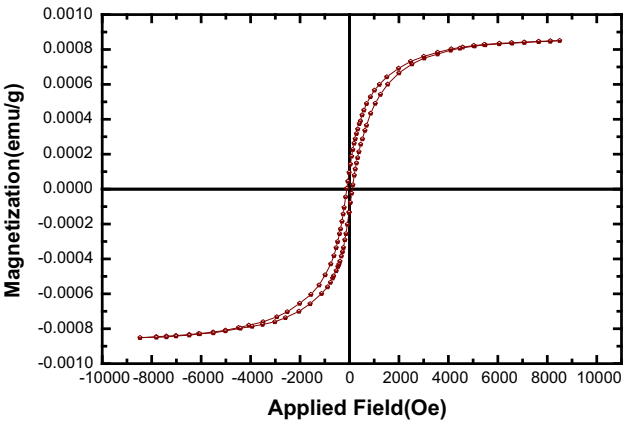

Fig. 4 VSM curves of $SrMoO_4$ nanostructures (sample 3)

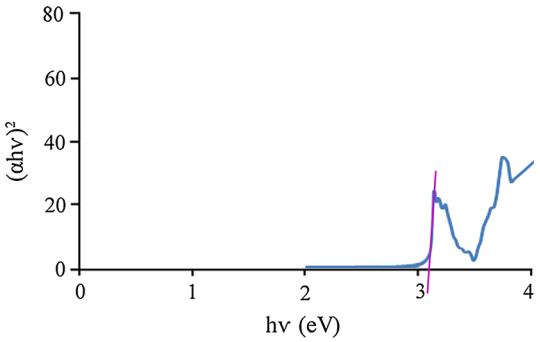

Fig. 5 UV–Vis pattern of $SrMoO_4$ nanostructures (sample 3)

numbers associated with the different types of electronic transitions. For n = 1/2, 2, 3/2 and 3, the transitions are directly allowed, indirectly allowed, directly forbidden, and indirectly forbidden, respectively. Each energy gap was determined by extrapolation of each linear portion of the

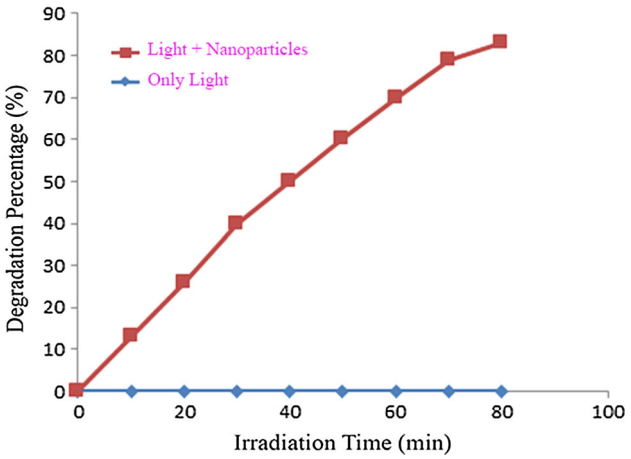

Fig. 6 Photocatalytic methyl orange degradation of $SrMoO_4$ nanostructures under ultraviolet light

curves to a = 0. In the present research, the $SrMoO_4$ presents directly allowed electronic transition (n = 1/2) and the energy gaps of $SrMoO_4$ nanostructures is 3.1 eV. Photodegradation of methyl orange (MO) as water contaminant under UV light illumination was employed to evaluate the properties of the as-synthesized $SrMoO_4$ nanostructures. Figure 6 exhibits the obtained result. No methyl orange was practically broken down after 80 min without employing UV light illumination or as-prepared nanostructures $SrMoO_4$. This observation illustrated that the contribution of self-degradation was insignificant. The proposed mechanism of the photocatalytic degradation of the methyl orange can be assumed as:

$$SrMoO_4 + h\nu \rightarrow SrMoO_4^{\cdot} + e^- + h^+ \quad (3)$$

$$h^+ + H_2O \rightarrow OH^{\cdot} \quad (4)$$

$$e^- + O_2 \rightarrow O_2^{\cdot -} \quad (5)$$

$$OH^{\cdot} + O_2^{\cdot} + \text{methyl orange} \rightarrow \text{Degradation products} \quad (6)$$

Utilizing photocatalytic calculations by Eq. (1), the methyl orange degradation was about 83 % after 80 min illumination of UV light in the presence of samples 3. This obtained result demonstrates that as-prepared $SrMoO_4$ nanostructures have high potential to be applied as favorable and appropriate material for photocatalytic applications under illumination of UV light. The heterogeneous photocatalytic processes have diffusion, adsorption and reaction steps. It has been shown that the desirable distribution of the pore has effective and important impact on the diffusion of the reactants and products, and therefore effects on the photocatalytic activity. It seems that the enhanced photocatalytic activity of the as-obtained nanostructures $SrMoO_4$ can be owing to desirable and appropriate distribution of the pore, high hydroxyl amount

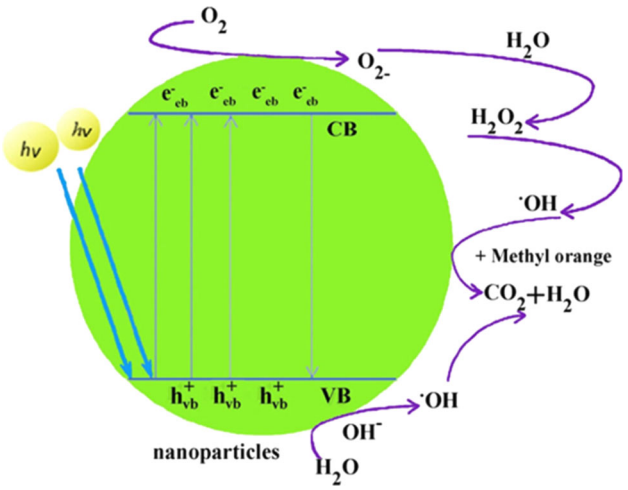

Scheme 1 Reaction mechanism of methyl orange photodegradation over $SrMoO_4$ nanostructures under UV light irradiation

and high separation rate of charge carriers (Scheme 1). Furthermore, this route is facile to operate and very suitable for industrial production of $SrMoO_4$ nanostructures.

4 Conclusions

In summary, a simple, inexpensive and single-step method has been developed for the synthesis of strontium molybdate ($SrMoO_4$) nanostructures. In this work, the crystallinity and morphology of $SrMoO_4$ have been controlled. To investigate the effect of capping agents on the morphology and size of final products several tests were performed in the presence of phenylalanine, glycine, and cysteine. VSM analyzes indicates a ferromagnetic behavior for the synthesized nanostructures. When as obtained $SrMoO_4$ nanoparticles was employed as photocatalyst, the percentage of the methyl orange degradation was about 83 % after 80 min irradiation of UV light. This result suggests as-synthesized strontium molybdate as interesting and favorable candidate for photocatalytic applications under UV light.

Acknowledgments Authors are grateful to council of University of Imam Hossein for providing financial support to undertake this work.

References

1. V. Arabali, M. Ebrahimi, M. Abbasghorbani, V. Kumar Gupta, M. Farsi, M.R. Ganjali, F. Karimi, J. Mol. Liq. **213**, 312 (2016)
2. H.R. Naderi, P. Norouzi, M.R. Ganjali, Appl. Surf. Sci. **366**, 552 (2016)
3. S.M. Hosseinpour-Mashkani, A. Sobhani-Nasab, J. Mater. Sci.: Mater. Electron. **27**, 3240 (2016)
4. M. Zahraei, A. Monshi, D. Shahbazi-Gahrouei, M. Amirnasr, B. Behdadfar, M. Rostami, J. Nanostruct. **5**, 137 (2015)

5. M. Rahimi-Nasrabadi, J. Nanostruct. **4**, 211 (2014)
6. M. Maddahfar, M. Ramezani, M. Sadeghi, A. Sobhani-Nasab, J. Mater. Sci.: Mater. Electron. **26**, 7745 (2015)
7. S. Khaleghi, J. Nanostruct. **2**, 157 (2012)
8. M. Aliahmad, A. Rahdar, Y. Azizi, J. Nanostruct. **4**, 145 (2014)
9. M. Enhessari, M. Kargar-Razi, P. Moarefi, A. Parviz, J. Nanostruct. **2**, 119 (2012)
10. M. Behpour, M. Mehrzad, S.M. Hosseinpour-Mashkani, J. Nanostruct. **5**, 183 (2015)
11. M. Ishii, M. Kobayashi, Prog. Cryst. Growth Charact. **23**, 245 (1991)
12. N. Faure, C. Borel, M. Couchaud, G. Basset, R. Templier, C. Wyon, Appl. Phys. B **63**, 593 (1996)
13. G. Angloher, C. Bucci, C. Cozzini, F. von Feilitzsch, T. Frank, D. Hauff, S. Henry, T.H. Jagemann, J. Jochum, H. Kraus, B. Majorovits, J. Ninkovie, F. Petricca, F. Probst, Y. Ramachers, W. Rau, W. Seidel, M. Stark, S. Uchaikin, L. Stodolsky, H. Wulandari, Nucl. Instrum. Methods Phys. Res. A **520**, 108 (2004)
14. E.F. Paski, M.W. Blades, Anal. Chem. **60**, 1224 (1988)
15. M. Daturi, L. Savary, G. Costentin, J.C. Lavalley, Catal. Today **61**, 231 (2000)
16. N. Sharma, K.M. Shaju, G.V. Subba Rao, B.V.R. Chowdari, Z.L. Dong, T.J. White, Chem. Inform. **15**, 101 (2004)
17. A. Brenier, G.H. Jia, C.Y. Tu, J. Phys. Condens. Matter **16**, 9103 (2004)
18. C. Pupp, R. Yamdagni, R.F. Porter, J. Inorg. Nucl. Chem. **31**, 2021 (1969)
19. Y. Sun, J. Ma, J. Fang, C. Gao, Z. Liu, Ceram. Int. **37**, 683 (2011)
20. C.T. Xia, V.M. Fuenzalida, R.A. Zarate, J. Alloys Compd. **316**, 250 (2001)
21. Y. Mi, Z.Y. Huang, F.L. Hu, X.Y. Li, Mater. Lett. **63**, 742 (2009)
22. A.P. de Azevedo Marques, D.M.A. de Melo, C.A. Paskocimas, P.S. Pizani, E.R. Joya, E.Longo Leite, J. Solid State Chem. **179**, 671 (2006)
23. C. Zhang, E.H. Shen, E.B. Wang, Z.H. Kang, L. Gao, C.W. Hu, L. Xu, Mater. Chem. Phys. **96**, 240 (2006)
24. P. Afanasiev, Mater. Lett. **61**, 4622 (2007)
25. J.H. Ryu, J.W. Yoon, C.S. Lim, K.B. Shim, Mater. Res. Bull. **40**, 1468 (2005)
26. M. Riazian, J. Nanostruct. **4**, 433 (2014)
27. M. Rahimi-Nasrabadi, M. Behpour, A. Sobhani-Nasab, S.M. Hosseinpour-Mashkani, J. Mater. Sci.: Mater. Electron. **26**, 9776 (2015)
28. S.M. Hosseinpour-Mashkani, M. Maddahfar, A. Sobhani-Nasab, J. Mater. Sci.: Mater. Electron. **27**, 474 (2016)
29. S.S. Hosseinpour-Mashkani, S.S. Hosseinpour-Mashkani, A. Sobhani-Nasab, J. Mater. Sci.: Mater. Electron. **27**, 4351 (2016)
30. J. Safaei-Ghomi, S. Zahedi, M. Javid, M.A. Ghasemzadeh, J. Nanostruct. **5**, 153 (2015)
31. M. Rahimi-Nasrabadi, S.M. Pourmortazavi, A. Akbar Davoudi-Dehaghani, S.S. Hajimirsadeghi, M.M. Zahedi, Cryst. Eng. Comm. **15**, 4077 (2013)
32. M. Behpour, M. Chakeri, J. Nanostruct. **2**, 227 (2012)
33. S.M. Pourmortazavi, M. Taghdiri, V. Makari, M. Rahimi-Nasrabadi, Spectrochim. Acta A Mol. Biomol. Spectrosc. **136**, 1249 (2015)
34. M. Rahimi-Nasrabadi, S.M. Pourmortazavi, M.R. Ganjali, Mater. Manuf. Process **30**, 34 (2015)
35. S.M. Pourmortazavi, M. Rahimi-Nasrabadi, S.S. Hajimirsadeghi, J. Dispers. Sci. Technol. **33**, 254 (2012)
36. S.M. Hosseinpour-Mashkani, M. Ramezani, A. Sobhani-Nasab, M. Esmaeili-Zare, J. Mater. Sci. Mater. Electron. **26**, 6086 (2015)
37. A. Sobhani-Nasab, M. Maddahfar, S.M. Hosseinpour-Mashkani, J. Mol. Liq. **216**, 1 (2016)
38. S.M. Pourmortazavi, M. Rahimi-Nasrabadi, M. Khalilian-Shalamzari, H.R. Ghaeni, S.S. Hajimirsadeghi, J. Inorg. Organomet. Polym. Mater. **24**, 333 (2014)
39. S. Khademolhoseini, M. Zakeri, S. Rahnamaeiyan, M. Nasiri, R. Talebi, J. Mater. Sci.: Mater. Electron. **26**, 7303 (2015)
40. R. Talebi, S. Khademolhoseini, S. Rahnamaeiyan, J. Mater. Sci.: Mater. Electron. **27**, 1427 (2016)
41. M. Rahimi-Nasrabadi, S.M. Pourmortazavi, M.R. Ganjali, S.S. Hajimirsadeghi, M.M. Zahedi, J. Mol. Struct. **1047**, 31 (2013)
42. S.M. Pourmortazavi, M. Rahimi-Nasrabadi, A.A. Davoudi-Dehaghani, A. Javidan, M.M. Zahedi, S.S. Hajimirsadeghi, Mater. Res. Bull. **47**, 1045 (2012)